Article

Thermally Induced Self-Assembly and Cyclization of -Leucyl--Leucine in Solid State

Marat A. Ziganshin, Aisylu S. Safiullina, Alexander Vladimirovich Gerasimov, Sufia A. Ziganshina, Alexander E. Klimovitskii, Khasan R. Khayarov, and Valery V. Gorbatchuk

J. Phys. Chem. B, **Just Accepted Manuscript** • DOI: 10.1021/acs.jpcb.7b06759 • Publication Date (Web): 18 Aug 2017

Thermally Induced Self-Assembly and Cyclization of L-Leucyl-L-Leucine in Solid State

Marat A. Ziganshin,[†] Aisylu S. Safiullina,[†] Alexander V. Gerasimov,[†] Sufia A. Ziganshina,[‡] Alexander E. Klimovitskii,[†] Khasan R. Khayarov,[†] and Valery V. Gorbatchuk,[†]*

[†] A.M. Butlerov Institute of Chemistry, Kazan Federal University, Kremlevskaya ul. 18, Kazan, 420008 Russia

[‡] Kazan Zavoisky Physical-Technical Institute of the Kazan Scientific Center of the Russian Academy of Sciences, Sibirskii trakt 10/7, Kazan, 420029 Russia

ABSTRACT: Thermal treatment of oligopeptides is one of the methods for synthesis of organic nanostructures. However, heating may lead not only to self-assembly of the initial molecules, but also to chemical reactions resulting in the formation of new unexpected nanostructures or change in the properties of the existing ones. In the present work, the reaction of cyclization of dipeptide $_{L}$-leucyl-$_{L}$-leucine in solid state under heating was studied. The change in morphology of dipeptide thin film and formation of nanostructures after heating was visualized using atomic force microscopy. This method also was used for demonstration of differences in self-assembly of linear and cyclic dipeptides. The chemical structure of reaction product was characterized by NMR spectrometry, FTIR spectroscopy and GC-MS analysis. Kinetic parameters of cyclization were estimated within the approaches of the non-isothermal kinetics ("model-free" kinetics and linear regression methods for detection of topochemical equation). The results of present work are useful for explanation the changes in the properties of nanostructures based on short-chain oligopeptides, notably leucyl-leucine, after thermal treatment, as well as for the synthesis of cyclic oligopeptides.

INTRODUCTION

Short-chain oligopeptides are popular objects for study at the present time, because of their potential advantages for various technologies.[1-3] They are used as supramolecular hosts[4-6] and microporous materials, which capable to selectively separate gas mixtures[7-9] and effectively bind organic molecules.[10,11] But the main reason for the increased interest in oligopeptides (mainly dipeptides) is their ability to self-assembly[12,13] with the formation of various nanostructures depending on the conditions.[14-18] Being biocompatible and environment-friendly oligopeptide-based materials are often considered as good alternatives to inorganic nanomaterials.[19-21]

There are several ways for preparation of oligopeptide nanostructures. The most common are the crystallization of oligopeptides from various solvents,[22,23] treatment of initially amorphous film with vapors at room temperature,[24,25] and thermal treatment, such as sublimation of oligopeptide powder in vacuum[26] or in inert gas atmosphere,[27] or heating of oligopeptide film with different vapors.[28] When using the heating method, one should take into account the possibility of chemical reaction in the oligopeptide phase and formation of new chemical compounds, for example, cyclic products.[29,30] As the result the formation of new type of nanostructures[14,26] or change in the properties of already existing nanostructures were observed.[31] For example, heating the leucyl-leucine based nanotubes to 180 °C leads to their transformation into wirelike fibrils and loss of nonlinear optical and piezoelectric properties, but the visible (blue and green) photoluminescence appears.[32,33]

Cyclization of dipeptides can occur both in solution,[34-36] and in the solid phase,[29,37] during the sublimation of powder,[27] even under impact of electron beam radiation in SEM experiments.[30] Cyclic dipeptides can form under heat treatment of protein foods, which leads to change in their taste,[38] or as side products in the synthesis of oligopeptides.[39,40] However, researchers do not

always consider the possibility of dipeptides cyclization in solid state, and explain the change in the properties of materials only as the result of phase transition under heating.

The cyclic oligopeptides are also the attractive objects of independent research[41], due to its advantages in comparison with the linear oligopeptides.[42] They are biologically active and can be used in medicine,[35,43,44] some of them show the catalytic activity.[45,46] Cyclic oligopeptides are used for preparation of organo- and hydrogels,[47,48] which can be useful for design of drug delivery systems and thermoresponsive smart materials.[49]

Thus, the study of the cyclization of short-chain oligopeptides induced by heating is of interest for the preparation of new useful compounds and organic nanostructures, and also for explanation of changes in the properties of peptide materials after the thermal treatment.

The present work is the first study of $_{L}$-leucyl-$_{L}$-leucine (Leu-Leu) cyclization in the solid state under heating. This reaction was studied using thermogravimetric analysis with simultaneous differential scanning calorimetry and mass-spectrometric detection of evolved vapors at different heating rates. The kinetic parameters of the reaction were calculated. The structure of formed *cyclo*(Leu-Leu) was characterized by ^{1}H and ^{13}C NMR spectroscopy, Fourier-transform infrared spectroscopy, GC-MS analysis. The self-assembly of Leu-Leu and *cyclo*(Leu-Leu) from hexafluoro-2-propanol as well as effect of thermal treatment on morphology of initial film of Leu-Leu were studied by atomic force microscopy.

EXPERIMENTAL

Materials. Dipeptide $_{L}$-leucyl-$_{L}$-leucine (Leu-Leu) (Bachem) and hexafluoro-2-propanol (Acros Organics #14754) were used without additional purification.

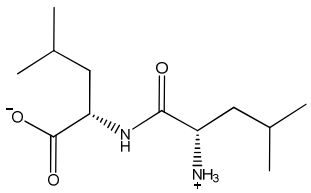

Leu-Leu

Thermoanalysis by Simultaneous TG/DSC/MS/. Simultaneous thermogravimetry (TG) and differential scanning calorimetry (DSC) analysis of dipeptide powder with mass spectrometric (MS) evolved gas analysis were performed using thermoanalyzer STA 449 C Jupiter (Netzsch) coupled with quadrupolar mass-spectrometer QMS 403C Aeolos (Netzsch) as described elsewhere.[50,51] For experiments, 4 mg samples of dipeptide were placed in aluminium crucibles (40 μl) with lids having 3 holes, each of 0.5 mm in diameter.

Kinetic Analysis of Cyclization of Leu-Leu. According to ICTAC recommendations, it is necessary to use at least two different kinetic computational methods.[52,53] The "model-free" methods for kinetic computations: ASTM E698, Ozawa-Flynn-Wall, and Friedman[54-58] were used. The same set of experimental data was used further for searching the topochemical equation as described in.[29,59] The data for kinetic analysis were obtained from TG data, measured at different heating rates: 2 K min^{-1}, 5 K min^{-1}, 10 K min^{-1}, 15 K min^{-1}. Calculations were performed using NETZSCH Thermokinetics 3.1.

^{1}H and ^{13}C NMR Spectroscopy. The NMR spectra were recorded on Bruker Avance III 400 spectrometer. ^{1}H NMR (400 MHz, DMSO-d_6, 25 °C). ^{13}C {^{1}H} NMR (100.6 MHz, DMSO-d_6, 25 °C).

Fourier-Transform Infrared (FTIR) Spectroscopy. FTIR spectra were collected using Bruker Vertex 70 FTIR spectrometer with a single reflection, germanium crystal ATR accessory (MIRacle, PIKE Technologies) with resolution of 2 cm^{-1} in dry air. All data were collected at 25 °C.

Atomic Force Microscopy (AFM). AFM images were recorded using the atomic force microscope Titanium (NT-MDT, Russia). Measurements were performed on air using a tapping mode. Revolution cartridge of cantilevers CNG (NT-MDT, Russia) was used. For AFM experiments, dipeptide films with diameter of 3 mm were prepared from hexafluoro-2-propanol solution (2 mg mL^{-1}) on the surfaces of highly oriented pyrolytic graphite (HOPG) plates (1×1 cm) as described in.[60] HOPG was freshly cleaved before use. All images were obtained at 298 K.

Gas Chromatography (GC) Mass Spectrometry (MS). GC-MS system including a gas chromatograph Chromatec-Crystal 5000 (Russia) with capillary column 30 m, 0.25 mm i.d. and mass spectrometry detector ISQ (Thermo Fisher Scientific) was used. Data were collected in the 0-600 m/z range at the following conditions: carrier gas was helium (velocity 1 mL min^{-1}), the injection port was maintained at 310 °C, temperature programs: from 100 °C to 150 °C at 12 °C min^{-1}, from 150 °C to 300 °C at 3 °C min^{-1}, electron ionization 70eV. The solution of dipeptide in hexafluoro-2-propanol (1 mg mL^{-1}) was used.

RESULTS AND DISCUSSION

Chemical Structure of Product of Thermal Treatment of Leu-Leu Powder. Earlier, we found the two steps on the TG curve associated with water loss under heating of Leu-Leu powder.[11] The first step of weight loss at 124 °C is the result of desorption of bound water. Heating of the Leu-Leu powder above 177 °C leads to appear the second step of mass loss on the TG curve which corresponds to evolve of 1 mol H_2O per mol dipeptide. This process is accompanied by an irreversible change in the packing of the dipeptide.[11] We proposed that the result of second step is formation of cyclic product *cyclo*(Leu-Leu) in accordance with scheme of reaction (Figure 1).

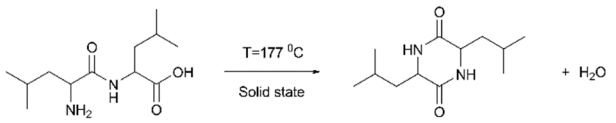

Figure 1. Scheme of the reaction of cyclization of Leu-Leu in the solid state.

To establish the chemical structure of the reaction product the ^{1}H and ^{13}C $\{^{1}H\}$ NMR spectrometry (Figure 2) and FTIR spectroscopy (Figure 3) were used. To this end, the Leu-Leu powder was heated up to 200 °C and NMR spectra were recorded for a solution of the reaction product in DMSO-d_6 (5 mg/mL).

Obtained data of NMR spectrometry (Figure 2) ^{1}H (δ = 0.86 (d, J = 6.5 Hz, 6H), 0.89 (d, J = 6.5 Hz, 6H), 1.42-1.49 (m, 2H), 1.55-1.62 (m, 2H), 1.76-1.84 (m, 2H), 3.70-3.74 (m, 2H), 8.22 (s, 2H)) and ^{13}C $\{^{1}H\}$ (δ = 22.2, 23.5, 24.1, 44.1, 53.2, 168.9) are in good correlation with the data for (3*S*,6*S*)-3,6-diisobutylpiperazine-2,5-dione (*cyclo*(Leu-Leu) synthesized in.[42,61]

Data of FTIR spectroscopy obtained for the powders of initial Leu-Leu, Leu-Leu after heating up to 140 °C and dipeptide powder after heating up 200 °C are presented in Figure 3.

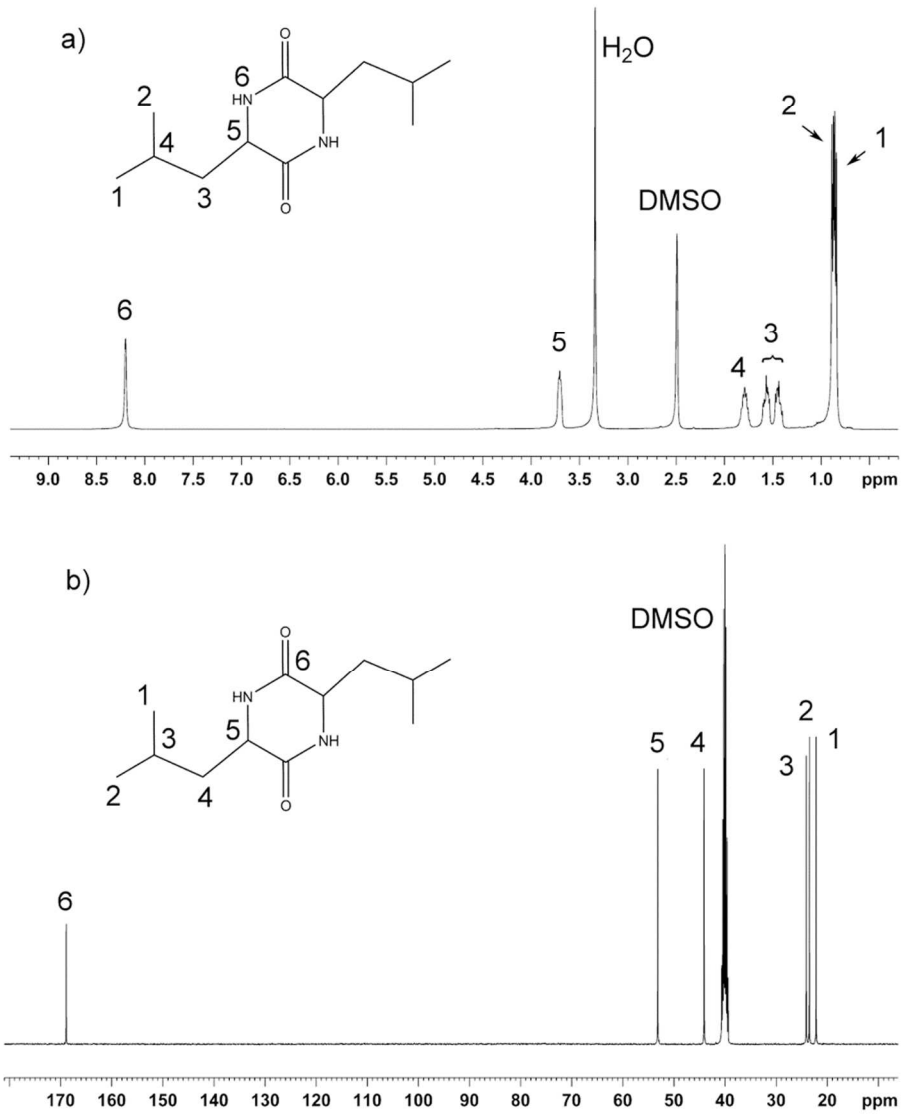

Figure 2. (a) ^{1}H NMR spectrum (400 MHz, DMSO-d_6) and (b) ^{13}C {^{1}H} NMR spectrum (100.6 MHz, DMSO-d_6) of *cyclo*(Leu-Leu).

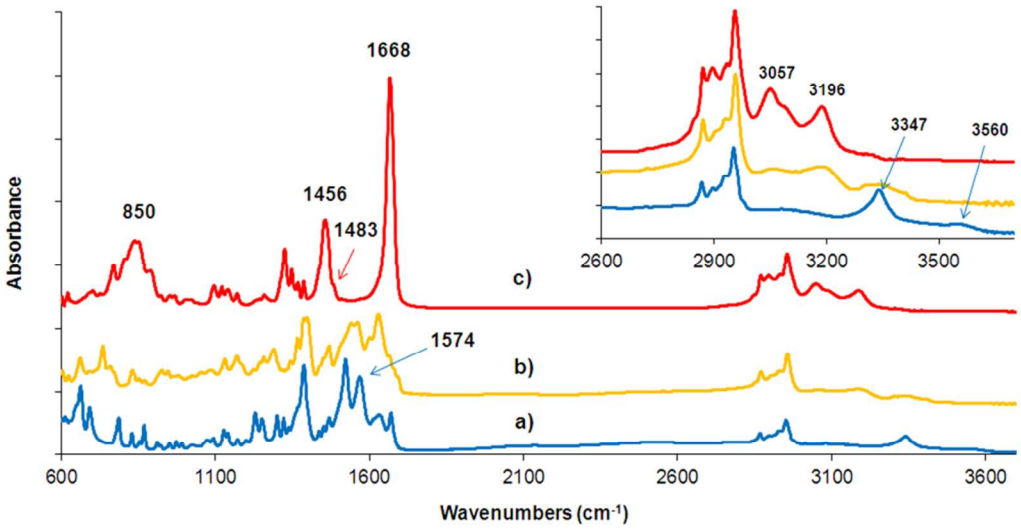

Figure 3. IR spectra at room temperature of powders of (a) initial Leu-Leu, (b) Leu-Leu after heating up to 145 °C and (c) Leu-Leu after heating up to 200 °C. The part of the spectrum in the range 2600-3700 cm^{-1} is shown in the inset.

The broad absorption band in FTIR spectra of initial powder Leu-Leu with a maximum at 3560 cm^{-1} is caused by the presence of water in dipeptide (Figure 3a). In the spectrum of the sample after heating up to 145 °C this band disappears (Figure 3b). The Red shift of N-H stretch band from 3347 cm^{-1}, Figure 3a, to 3196 cm^{-1} (Figure 3b) with simultaneous broadening after heating up to 145 °C may indicates the formation of additional H-bonds with the participation of the amide N-H group. For example, this group does not form H-bonds with >C=O group in clathrate with water,[62] but associated with carbonyl group of other dipeptide molecule in clathrates with alcohols.[63]

Analysis of the IR spectra obtained indicates a significant distinction of Leu-Leu heated to 200 °C compared to the other two studied samples. A more symmetric cyclic structure (Figure 1) of product heated up to 200 °C is in good agreement with the decrease in the number of absorption bands in the FTIR spectrum (Figure 3c) as compared to the spectrum of initial dipeptide (Figure

3a). The spectra of the initial dipeptide and sample heated up to 140 °C have absorption bands in the range 1500-1600 cm^{-1}, which correspond to the carboxyl and ammonium groups, as well as to the Amide II bands. The band at 1574 cm^{-1} (Figure 3a) is characteristic of a carboxylate anion ($–COO^-$)[64]. In the spectrum of *cyclo*(Leu-Leu) these bands are absent (Figure 3c). In the spectra of 2,5-diketopiperazines the Amide II region corresponding to deformation vibrations of N–H groups and stretching vibrations of the amide carbonyl groups are also absent.[65] A relatively intense absorption band at 1456 cm^{-1} observed in the spectrum of the sample heated up to 200 °C apparently is due to degenerate vibrations of alkyl groups because of symmetrical structure of this molecule. The shoulder at 1483 cm^{-1} may be related to in-plane bend of N–H group in the cycle.[66] A sharp peak at 1668 cm^{-1} (Amide I region) is corresponding to the amide carbonyl >C=O stretching frequency, which relates to a β-turn conformation (Figure 3c). The N–H out-plane bending appears at 850 cm^{-1} (Figure 3c).[67] The bands at 3057 and 3196 cm^{-1} apparently correspond to two N-H groups (in *cis*-configuration) which form H-bonds with the carbonyl groups of other molecules of *cyclo*(Leu-Leu).[67] The shoulder at 3091 cm^{-1} may be assign to the combination band of the C=O stretching and N-H in-plane vibrations of the *cis* CONH group.[67]

According to data of GC-MS the powder of Leu-Leu heated up to 200 °C contains one component (Figure 4a) for which the mass spectrum (Figure 4b) is in a good agreement with the MS data for 3,6-diisobutylpiperazine-2,5-dione[68].

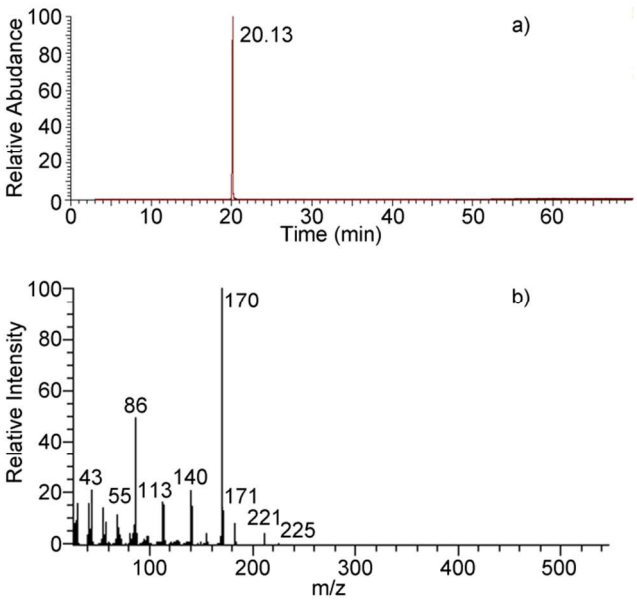

Figure 4. GC-MS of thermally induced powder of Leu-Leu up to 200 °C. (a) Data of GC, (b) data of MS.

So, analysis of NMR, IR and GC-MS data proves the formation of *cyclo*(Leu-Leu) after heating of initial dipeptide powder up to 200 °C.

Kinetic Analysis of Cyclization of Leu-Leu. A kinetic analysis of cyclization of Leu-Leu in the solid state was carried out for second step of mass lose, (Figure 5). The data for kinetic analysis were obtained from TG curves (Figure 5a) measured at different heating rates: 2, 5, 10 and 15 K min^{-1}.

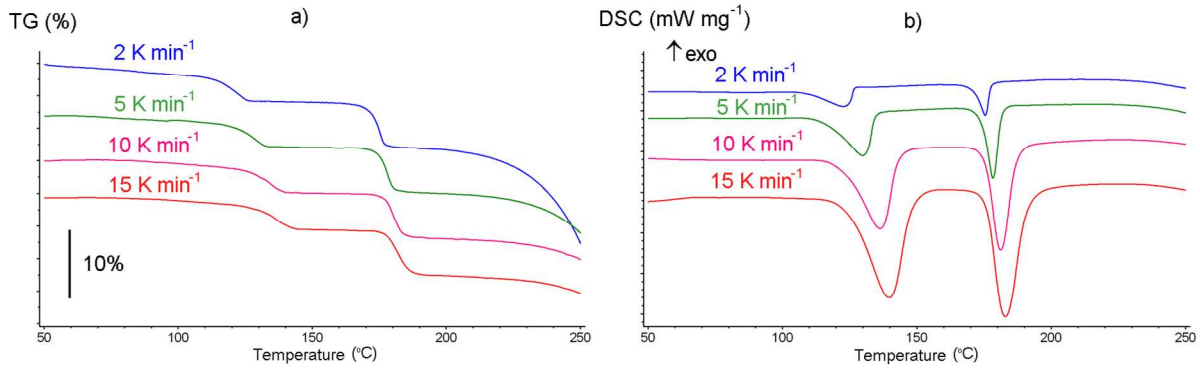

Figure 5. Data of (a) TG and (b) DSC analysis for Leu-Leu at different heating rates.

Calculations of activation energies were made for selected temperature intervals: from 160.4 to 183.3 °C for heating rate of 2 K min^{-1}, from 163.7 to 186.9 °C for heating rate of 5 K min^{-1}, from 167.0 to 190.2 °C for heating rate of 10 K min^{-1} and from 169.3 to 194.6 °C for heating rate of 15 K min^{-1}.

According to ASTM E698 analysis, the value of activation energy is E_a = 502 ± 11 kJ mol^{-1} and logarithm of Arrhenius constant is lg$A$ = 56.4. The Friedman analysis of reaction of Leu-Leu cyclization is shown in Figure 6. The obtained data indicate a complex character of the process studied. The higher slope of the experimental data compared with the *iso*-conversion lines at the beginning of the reaction indicates the autocatalytic process (Figure 6a). One can assume that the catalyst can be *cyclo*(Leu-Leu), for which the ability to catalyze the reaction of epoxidation was shown earlier.[46] According to Friedman method (Figure 6b) the value of activation energy is E_a = 519.5 ± 13.2 kJ mol^{-1} and logarithm of Arrhenius constant is lg$A$ = 58.4, whereas Ozawa–Flynn–Wall method gives E_a = 425.1 ± 23.3 kJ mol^{-1} and lg$A$ = 47.2. Data were obtained at conversion degree 0.2.

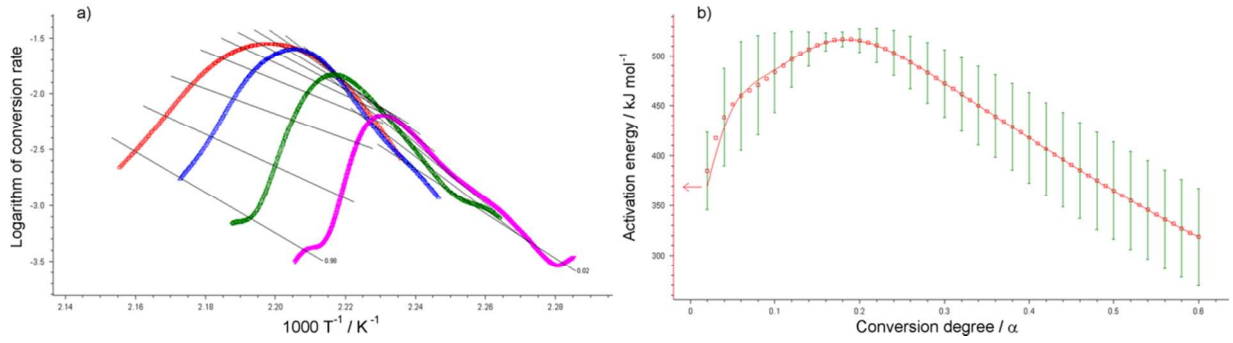

Figure 6. Friedman analysis of reaction of cyclization of Leu-Leu: (a) correlation of logarithm of conversion rate versus reciprocal temperature and (b) activation energies E_a versus degree of conversion α. Perpendicular lines show SD of calculation.

In accordance with *F* test, the best topochemical equation for the cyclization is CnB, which is used to describe the *n*th-order reaction with autocatalysis. The kinetic parameters calculated by using this model, as well as statistical quality parameters, are given in Table 1. Also, the data for the closest-quality model Bna, which is Prout-Tompkins equation with autocatalysis, are shown in Table 1. The correlation of experimental points from TG curves with the calculated lines in

Table 1. **Kinetic Parameters of Reaction of Leu-Leu Cyclization and Statistical Parameters of Calculation**[a]

Equation A →B	F_{exp}	F_{crit}	F_{act}	E_a / kJ mol^{-1}	lg$A$	Reaction order	Corr. coeff.
CnB	1.00	1.05	3494	434.1±0.7	48.0±0.07	1.46	0.998994
Bna	1.22	1.05	3494	431.2±1.6	48.5±0.18	1.05	0.998601

[a] The used topochemical equations are *n*th-order reaction with autocatalysis through the reactants (CnB) and Prout–Tompkins (Bna).[69] Data on the *F* test of fit quality (to identify the best kinetic description).

accordance with equation CnB is shown in Figure 7. From the viewpoints of thermodynamics, the revealed autocatalytic mechanism of this reaction may be caused not only by the decrease in the activation energy after accumulation of enough amount of the cyclic product (Figure 6b), which can act as catalyst in this reaction. But also as the result of decrease of system energy due to formation of at least two intermolecular hydrogen bonds per molecule of *cyclo*(Leu-Leu) (Figure 3) and to participation of alkyl groups in hydrophobic interactions.

The obtained values of activation energy, Arrhenius constant and reaction order are in good compliance with the calculated ones by Ozawa–Flynn–Wall approach. Thus, these kinetic parameters may be used to describe the reaction of cyclization of $_L$-leucyl-$_L$-leucine in solid phase.

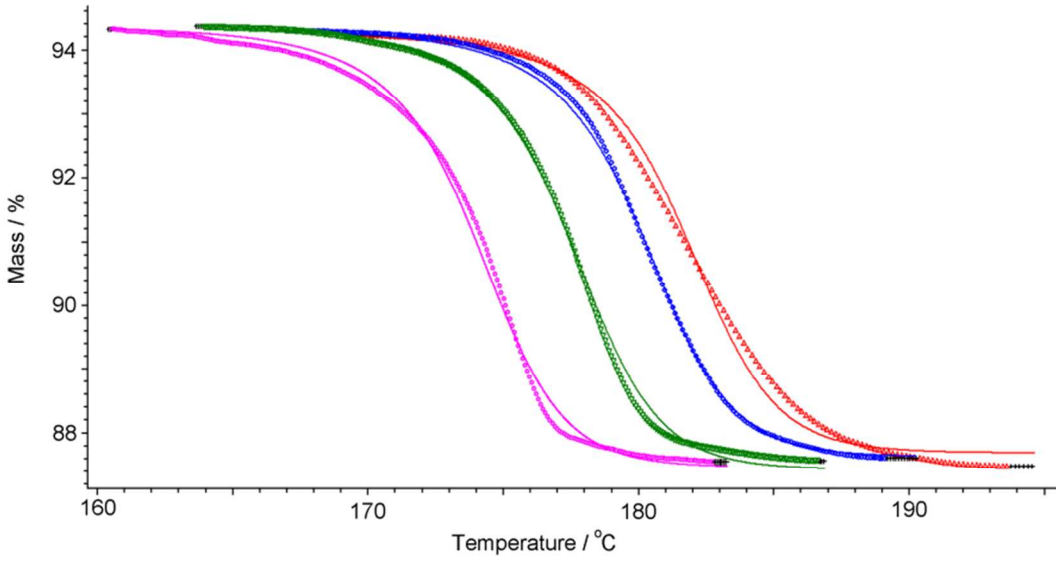

Figure 7. Correlation of experimental points from TG curves with the calculated lines in accordance with equation CnB.

It should be noted that the obtained values of activation energy for studied reaction are relatively large. For example, this value for solid phase cyclization of diphenylalanine, which starts at 147 °C, is 148 kJ mol^{-1}.[29] One can assume that the formation of intermolecular H-bond between >N-H and >C=O groups of different Leu-Leu molecules after water desorption (Figure 3b) can hinder the intramolecular cyclization, and increase the value of activation energy.

AFM Study of Surface Morphology. We visualized the effect of temperature on the state of dipeptide film. For this the AFM images of the films of initial Leu-Leu from the hexafluoro-2-propanol (HFIP) solution, and Leu-Leu films after sequential heating to 145 °C and 200 °C were obtained (Figure 8). Also the AFM image of film of *cyclo*(Leu-Leu) from solution in HFIP was obtained (Figure 10). The powder of *cyclo*(Leu-Leu) was prepared as described in Figure 1.

Amorphous and relatively smooth film of dipeptide is formed on the surface of HOPG after solvent (HFIP) has been removed (Figure 8a). The average height spread on a 10×10 μm scan was 13 nm. A mean square roughness of the surface (R_q) was 2 nm. After heating up to 145 °C

the morphology of the initial film changed (Figure 8b). The chaotically located objects, similar to short-hairs with length of 240-600 nm, were appeared on the film surface. The mean square roughness of the surface increased to 3.4 nm. One can assume that the driving force of observed self-assembly of the dipeptide molecules is the formation of additional intermolecular hydrogen bonds after water release (Figure 3b).

As a result of further film heating up to 200 °C, the flat plates with width of 200-300 nm, thickness of 30-70 nm, and length of more than 1000 nm were formed on its surface (Figure 8c). A mean square roughness of the surface (R_q) was 21.4 nm. The scheme of possible molecular organization of *cyclo*(Leu-Leu) in solid phase after heating is shown in Figure 9.

The similar structures were found after the crystallization from HFIP solution of *cyclo*(Leu-Leu) (Figure 10). In the last case, the length, width and height of the flat plates were 0.5-2.4 μm, 100-470 nm and 10-35 nm, correspondingly.

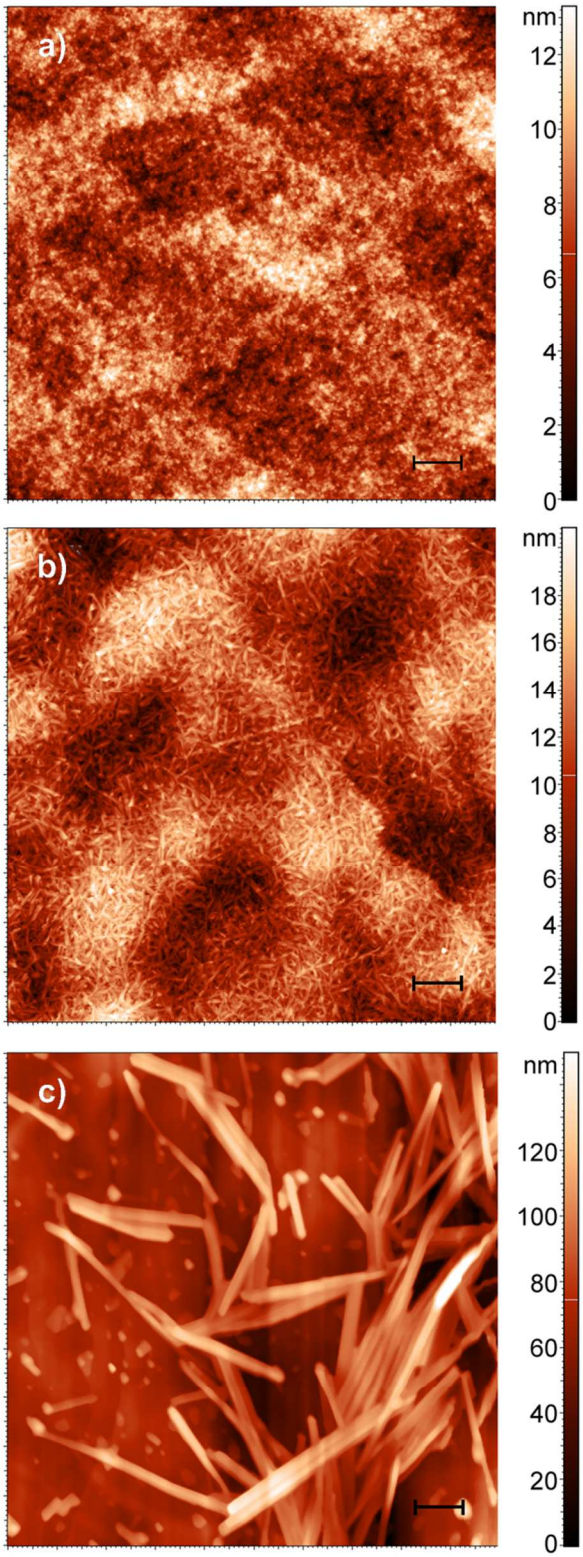

Figure 8. AFM images of the surface of (a) the initial Leu-Leu film deposited on the HOPG surface from a HFIP solution, (b) Leu-Leu film after heating up to 145 °C, (c) Leu-Leu film after

heating up to 200 °C. Scale bar = 1 μm.

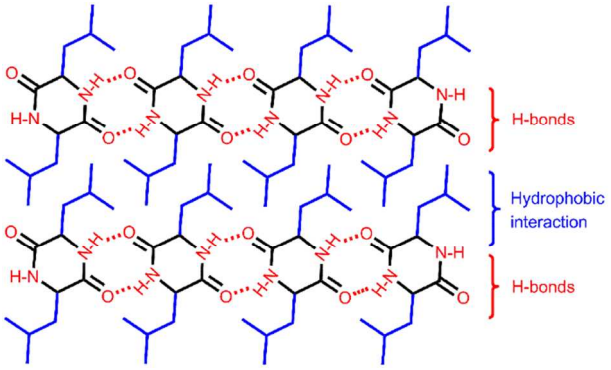

Figure 9. Scheme of possible organization of *cyclo*(Leu-Leu) in solid phase.

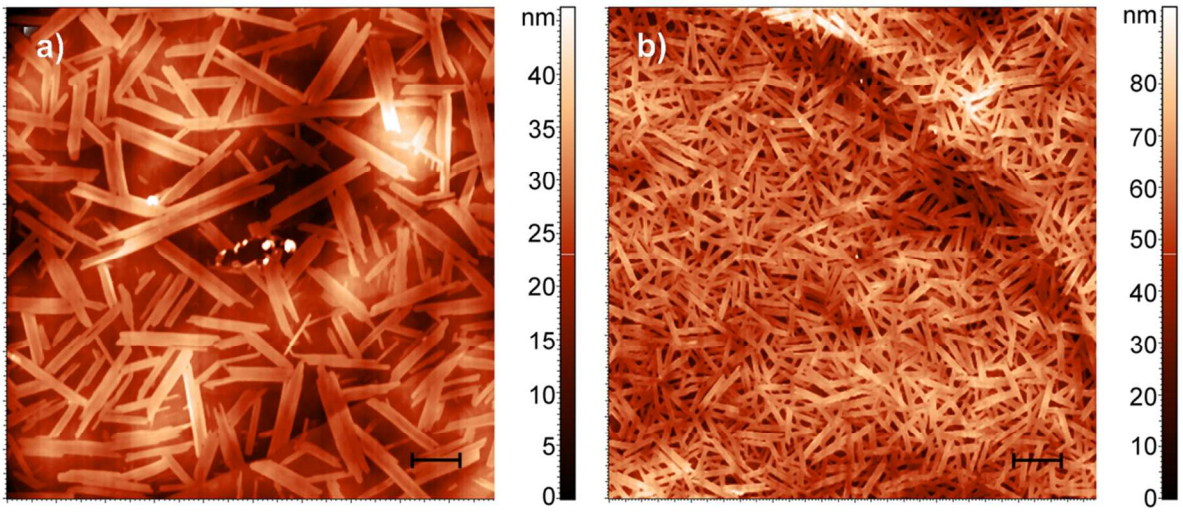

Figure 10. AFM images of the surface of film with the nanostructures obtained from solution of *cyclo*(Leu-Leu) in HFIP with different magnification. Scale bar = 3 μm (a) and 1 μm (b).

We believe that self-assembly of *cyclo*(Leu-Leu) in such practically two-dimensional elongated objects is due to formation of the four hydrogen bonds per each molecule of dipeptide (Figure 9), which leads to the formation of molecular chains in solid phase.[70]

CONCLUSION

The solid-phase reaction of $_{L}$-leucyl-$_{L}$-leucine cyclization was studied in the course of thermal analysis. The heating of the dipeptide powder above 177 °C leads to formation of cyclic dipeptide, which structure was confirmed by ^{1}H, ^{13}C NMR, Fourier-transform infrared spectroscopy and GC-MS analysis. Studied reaction of solid phase cyclization of $_{L}$-leucyl-$_{L}$-leucine is a complex reaction with autocatalysis. The calculated kinetic parameters of this reaction are E_a = 434 kJ mol-1, lg$A$ = 48, and the reaction order is close to 1.5. The relatively high calculated value of the activation energy may be a consequence of $_{L}$-leucyl-$_{L}$-leucine self-assembly through the formation of additional intermolecular hydrogen bonds. As a result of this process, the small hairs-like objects (length less than 600 nm) are formed on the surface of dipeptide film, concurrent with the red shift of N-H stretch band observed in the IR spectrum. Probably, this self-assembly complicates the "folding" of dipeptide molecule which necessary to start of intramolecular reaction.

The cyclization of $_{L}$-leucyl-$_{L}$-leucine in the solid phase leads to formation of elongate 2D plates, the same objects are observed when cyclic dipeptide crystallized from the polar H-donor hexafluoro-2-propanol on the surface of hydrophobic pyrolytic graphite. While the linear $_{L}$-leucyl-$_{L}$-leucine forms a smooth amorphous film under the same conditions.

The results of present work explain the changes in the properties of nanostructures based on leucyl-leucine after heating, and also can be used for further development of techniques for the preparation of nanomaterials based on oligopeptides.

AUTHOR INFORMATION

Corresponding Author

* E-mail: Marat.Ziganshin@kpfu.ru (M.A.Z.). Phone: +784322337309

Notes

The authors declare no competing financial interest.

ACKNOWLEDGEMENTS

This work was supported by the Ministry of Education and Science of Russian Federation [grant №14.Y26.31.0019].

REFERENCES

(1) Busseron, E.; Ruff, Y.; Moulin E.; Giuseppone, N. Supramolecular Self-Assemblies as Functional Nanomaterials. *Nanoscale*. **2013**, *5*, 7098–7140.

(2) Hamley, I. W. Peptide Nanotubes. *Angew. Chem., Int. Ed.* **2014**, *53*, 6866–6881.

(3) Ma, H.; Fei, J.; Li Q.; Li, J. Photo-Induced Reversible Structural Transition of Cationic Diphenylalanine Peptide Self-Assembly. *Small* **2015**, *11*, 1787–1491.

(4) Gorbitz, C. H. An Exceptionally Stable Peptide Nanotube System with Flexible Pores. *Acta Crystallogr., Sect. B: Struct. Sci.* **2002**, *58*, 849–854.

(5) Burchell, T. J.; Soldatov, D. V.; Enrighta G. D.; Ripmeester, J. A. The Ability of Lower Peptides to Form Co-Crystals: Inclusion Compounds of Leu-Leu-Leu Tripeptide with Pyridine and Picolines. *CrystEngComm*. **2007**, *9*, 922–929.

(6) Akazome, M.; Doba, A.; Matsumoto, S.; Ogura, K. Predominant (S)-Enantioselective Inclusion of Aryl Methyl Sulfoxides by (S)-Isoleucyl-(S)-Phenylglycines. *J. Org. Chem.* **2010**, *75*, 660–665.

(7) Comotti, A.; Bracco, S.; Distefano, G.; Sozzani, P. Methane, Carbon Dioxide and Hydrogen Storage in Nanoporous Dipeptide-Based Materials. *Chem. Commun.* **2009**, *3*, 284–286.

(8) Afonso, R. V.; Durao, J.; Mendes, A.; Damas, A. M.; Gales, L. Dipeptide Crystals as Excellent Permselective Materials: Sequential Exclusion of Argon, Nitrogen, and Oxygen. *Angew. Chem., Int. Ed.* **2010**, *49*, 3034–3036.

(9) Afonso, R.; Mendes, A.; Gales, L. Hydrophobic Dipeptide Crystals: a Promising Ag-Free Class of Ultramicroporous Materials Showing Argon/Oxygen Adsorption Selectivity. *Phys. Chem. Chem. Phys*. **2014**, *16*, 19386–19393.

(10) Ziganshin, M. A.; Gubina, N. S.; Gerasimov, A. V.; Gorbatchuk, V. V.; Ziganshina, S. A.; Chuklanov, A. P.; Bukharaev, A. A. Interaction of L-alanyl-L-valine and L-valyl-L-alanine with Organic Vapors: Thermal Stability of Clathrates, Sorption Capacity and the Change in the Morphology of Dipeptide Films. *Phys. Chem. Chem. Phys*. **2015**, *17*, 20168–20177.

(11) Ziganshin, M. A.; Safiullina, A. S.; Ziganshina, S. A.; Gerasimov, A. V.; Gorbatchuk, V.V. Non-Zeolitic Properties of the Dipeptide L-leucyl-L-leucine as a Result of the Specific Nanostructures Formation. *Phys. Chem. Chem. Phys.* **2017**, *19*, 13788–13797.

(12) Yuan, Ch.; Li, Sh.; Zou, Q.; Ren, Y.; Yan, X. Multiscale Simulations for Understanding of Evolution and Mechanism of Hierarchical Peptide Self-Assembly. *Phys. Chem. Chem. Phys.* **2017**, DOI: 10.1039/C7CP01923H.

(13) Naskar, J.; Roy, S.; Joardar, A.; Das, S.; Banerjee, A. Self-Assembling Dipeptide-Based Nontoxic Vesicles as Carriers for Drugs and Other Biologically Important Molecules. *Org. Biomol. Chem.* **2011**, *9*, 6610–6615.

(14) Ryu, J.; Park, C. B. High Stability of Self-Assembled Peptide Nanowires Against Thermal, Chemical, and Proteolytic Attacks. *Biotechnol. Bioeng.* **2010**, *105*, 221–230.

(15) Ziganshin, M. A.; Gubina, N. S.; Gorbatchuk, V. V.; Ziganshina, S. A.; Chuklanov, A. P.; Bizyaev, D. A.; Bukharaev, A. A. AFM Study of Thin Films of Oligopeptide L-valyl-L-valine

before and after Interaction with Vapors. *J. Surf. Invest.: X-Ray, Synchrotron Neutron Tech.* **2016**, *10*, 210–216.

(16) Xie, M.; Li, H.; Ye, M.; Zhang, Y.; Hu, J. Self-Assembly on Mica under Ethanol-Containing Atmospheres: Effects of Ethanol on Epitaxial Growth of Peptide Nanofilaments. *J. Phys. Chem. B*. **2012**, *116*, 2927–2933.

(17) Liu, X.; Fei, J.; Wang, A.; Cui, W.; Zhu, P.; Li, J. Transformation of Dipeptide-Based Organogels into Chiral Crystals by Cryogenic Treatment. *Angew. Chem. Int. Ed*. **2017**, *56*, 2660–2663.

(18) Wang, J.; Liu, K.; Xinga, R.; Yan, X. Peptide Self-Assembly: Thermodynamics and Kinetics. *Chem. Soc. Rev.* **2016**, *45*, 5589–5604.

(19) Gorbitz, C. H. Microporous Organic Materials from Hydrophobic Dipeptides. *Chem. - Eur. J.* **2007**, *13*, 1022–1031.

(20) Afonso, R.; Mendes, A.; Gales, L. Peptide-Based Solids: Porosity and Zeolitic Behavior. *J. Mater. Chem.* **2012**, *22*, 1709–1723.

(21) Zou, Q.; Abbas, M.; Zhao, L.; Li, S.; Shen, G.; Yan, X. Biological Photothermal Nanodots Based on Self-Assembly of Peptide−Porphyrin Conjugates for Antitumor Therapy. *J. Am. Chem. Soc.* **2017**, *139*, 1921−1927.

(22) Li, H.; Zhang, F.; Zhang, Y.; He, J.; Hu, J. Organic Solvents Mediate Self-Assembly of GAV-9 Peptide on Mica Surface. *Acta Biochim. Biophys. Sin.* **2007**, *39*, 285–289.

(23) Ariga, K.; Kikuchi, J.; Naito, M.; Koyama, E.; Yamada, N. Modulated Supramolecular Assemblies Composed of Tripeptide Derivatives: Formation of Micrometer-Scale Rods,

Nanometer-Size Needles, and Regular Patterns with Molecular-Level Flatness from the Same Compound. *Langmuir*. **2000**, *16*, 4929–4939.

(24) Ryu, J.; Park, C. B. Solid-Phase Growth of Nanostructures from Amorphous Peptide Thin Film: Effect of Water Activity and Temperature. *Chem. Mater.* **2008**, *20*, 4284–4290.

(25) Efimova, I. G.; Ziganshin, M. A.; Gorbatchuk, V. V.; Soldatov, D. V.; Ziganshina, S. A.; Chuklanov, A. P.; Bukharaev, A. A. Formation of Nanoislands on the Surface of Thin Dipeptide Films under the Effect of Vaporous Organic Compounds. *Prot. Met. Phys. Chem. Surf.* **2009**, *45*, 525–528.

(26) Adler-Abramovich, L.; Aronov, D.; Beker, P.; Yevnin, M.; Stempler, Sh.; Buzhansky, L.; Rosenman, G.; Gazit, E. Self-Assembled Arrays of Peptide Nanotubes by Vapour Deposition. *Nat. Nanotechnol.* **2009**, *4*, 849–854.

(27) Lee, J. S.; Yoon, I.; Kim, J.; Ihee, H.; Kim, B.; Park, C. B. Self-Assembly of Semiconducting Photoluminescent Peptide Nanowires in the Vapor Phase. *Angew. Chem., Int. Ed.* **2011**, *50*, 1164–1167.

(28) Ryu, J.; Park, C. B. High-Temperature Self-Assembly of Peptides into Vertically Well-Aligned Nanowires by Aniline Vapor. *Adv. Mater.* **2008**, *20*, 3754–3758.

(29) Ziganshin, M. A.; Gerasimov, A. V.; Ziganshina, S. A.; Gubina, N. S.; Abdullina, G. R.; Klimovitskii, A. E.; Gorbatchuk, V. V.; Bukharaev, A. A. Thermally Induced Diphenylalanine Cyclization in Solid Phase. *J. Therm. Anal. Calorim.* **2016**, *125*, 905–912.

(30) Amdursky, N.; Beker, P.; Koren, I.; Bank-Srour, B.; Mishina, E.; Semin, S.; Rasing, T.; Rosenberg, Y.; Barkay, Z.; Gazit, E.; et al. Structural Transition in Peptide Nanotubes. *Biomacromolecules*. **2011**, *12*, 1349–1354.

(31) Heredia, A.; Bdikin, I.; Kopyl, S.; Mishina, E.; Semin, S.; Sigov, A.; German, K.; Bystrov, V.; Gracio, J.; Kholkin, A. L. Temperature-Driven Phase Transformation in Self-Assembled Diphenylalanine Peptide Nanotubes. *J. Phys. D: Appl. Phys.* **2010**, *43*, 462001 (6 pp).

(32) Handelman, A.; Natan, A.; Rosenman, G. Structural and Optical Properties of Short Peptides: Nanotubes-to-Nanofibers Phase Transformation. *J. Pept. Sci.* **2014**, *20*, 487–493.

(33) Handelman, A.; Kuritz, N.; Natan, A.; Rosenman, G. Reconstructive Phase Transition in Ultrashort Peptide Nanostructures and Induced Visible Photoluminescence. *Langmuir*. **2016**, *32*, 2847–2862.

(34) Exner, M. M.; Kostelnik, R. Synthesis and Carbon-13 Nuclear Magnetic Resonance Spectra of Cyclo(D-leucyl-L-leucine) and Cyclo(L-leucyl-L-leucine). *Biopolymers.* **1977**, *16*, 1387–1395.

(35) Borthwick, A. D. 2,5-Diketopiperazines: Synthesis, Reactions, Medicinal Chemistry, and Bioactive Natural Products. *Chem. Rev.* **2012**, *112*, 3641–3716.

(36) Li, Y.; Yan, L.; Liu, K.; Wang, J.; Wang, A.; Bai, S.; Yan, X. Solvothermally Mediated Self-Assembly of Ultralong Peptide Nanobelts Capable of Optical Waveguiding. *Small.* **2016**, *12*, 2575–2579.

(37) Zelenovskiy, P. S.; Davydov, A. O.; Krylov, A. S.; Kholkin, A. L. Raman Study of Structural Transformations in Self-Assembled Diphenylalanine Nanotubes at Elevated Temperatures. *J. Raman Spectrosc.* **2017**, doi: 10.1002/jrs.5084.

(38) Borthwick, A. D.; Da Costa, N. C. 2,5-Diketopiperazines in Food and Beverages: Taste and Bioactivity. *Crit. Rev. Food Sci. Nutr.* **2017**, *57*, 718–742.

(39) Wei, Y.; Pei, D. Activation of Antibacterial Prodrugs by Peptide Deformylase. *Bioorg. Med. Chem. Lett.* **2000**, *10*, 1073–1076.

(40) Anne, C.; Fournié-Zaluski, M.-C.; Roques, B. P.; Cornille, F. Solid Phase Synthesis of Peptoid Derivatives Containing a Free C-Terminal Carboxylate. *Tetrahedron Lett.* **1998**, *39*, 8973–8974.

(41) Carvajal-Diaz, J. A.; Cagin, T. Electrophoretic Transport of Na+ and K+ Ions within Cyclic Peptide Nanotubes. *J. Phys. Chem. B*. **2016**, *120*, 7872−7879.

(42) Manchineella, S.; Govindaraju, T. Molecular Self-Assembly of Cyclic Dipeptide Derivatives and Their Applications. *ChemPlusChem*. **2017**, *82,* 88–106.

(43) Rhee, K.-H. Cyclic Dipeptides Exhibit Synergistic, Broad Spectrum Antimicrobial Effects and have Anti-Mutagenic Properties. *Int. J. Antimicrob. Agents*. **2004**, *24*, 423–427.

(44) Madhu, C.; Voshavar, C.; Rajasekhar, K.; Govindaraju, T. Cyclic Dipeptide Based Cell-Penetrating Peptidomimetics for Effective DNA Delivery. *Org. Biomol. Chem.* **2017**, *15*, 3170–3174.

(45) Bérubé, C.; Voyer, N. Biomimetic Epoxidation in Aqueous Media Catalyzed by Cyclic Dipeptides. *Synth. Commun.* **2016**, *46*, 395–403.

(46) Bérubé, C.; Barbeau, X.; Cardinal, S.; Boudreault, P.-L.; Bouchard, C.; Delcey, N.; Lagüe, P.; Voyer, N. Interfacial Supramolecular Biomimetic Epoxidation Catalysed By Cyclic Dipeptides. *Supramol. Chem.* **2017**, *29*, 330–349.

(47) Xie, Z.; Zhang, A.; Ye, L.; Feng, Z. Organo- and Hydrogels Derived from Cyclo(L-Tyr-L-Lys) and its 3-Amino Derivatives. *Soft Matter*. **2009**, *5*, 1474–1482.

(48) Geng, H.; Ye, L.; Zhang, A.; Li, J.; Feng, Z. Low-Molecular-Weight Organo- and Hydrogelators Based on Cyclo(L-Lys-L-Glu). *Langmuir*. **2016**, *32*, 4586–4594.

(49) Manchineella, S.; Govindaraju, T. Hydrogen Bond Directed Self-Assembly of Cyclic Dipeptide Derivatives: Gelation and Ordered Hierarchical Architectures. *RSC Adv.* **2012**, *2*, 5539–5542.

(50) Yakimova, L. S.; Ziganshin, M. A.; Sidorov, V. A.; Kovalev, V. V.; Shokova, E. A.; Tafeenko, V. A.; Gorbatchuk, V. V. Molecular Recognition of Organic Vapors By Adamantylcalix[4]arene in QCM Sensor Using Partial Binding Reversibility. *J. Phys. Chem. B.* **2008**, *112*, 15569–15575.

(51) Ziganshin, M. A.; Gerasimov, A. V.; Gorbatchuk, V. V.; Gubaidullin, A. T. Thermal Analysis of Clathrates of Tripeptide LLL with Organic Compounds and Water. *J. Therm. Anal. Calorim.* **2015**, *119*, 1811–1816.

(52) Vyazovkin, S.; Burnham, A. K.; Criado, J. M.; Luis, A.; Perez-Maqueda, L. A.; Popescu, C.; Sbirrazzuoli, N. ICTAC Kinetics Committee Recommendations for Performing Kinetic Computations on Thermal Analysis Data. *Thermochim. Acta.* **2011**, *520*, 1–19.

(53) Vyazovkin, S.; Chrissafis, K.; Di Lorenzo, M.-R.; Koga, N.; Pijolat, M.; Roduit, B.; Sbirrazzuoli, N.; Suñol, J.-J. ICTAC Kinetics Committee Recommendations for Collecting Experimental Thermal Analysis Data for Kinetic Computations. *Thermochim. Acta.* **2014**, *590*, 1–23.

(54) Kissinger, H. E. Variation of Peak Temperature with Heating Rate in Differential Thermal Analysis. *J. Res. Natl. Bur. Stand.* (*U. S.*). **1956**, *57*, 217–221.

(55) Friedman, H. L. Kinetics of Thermal Degradation of Charforming Plastics from Thermogravimetry. Application to a Phenolic Plastic. *J. Polym. Sci.* **1964**, *6*, 183–195.

(56) Ozawa, T. A New Method of Analyzing Thermogravimetric Data. *Bull. Chem. Soc. Jpn.* **1965**, *38*, 1881–1886.

(57) Ozawa, T. Estimation of Activation Energy by Isoconversion Methods. *Thermochim. Acta*. **1992**, *203*, 159–165.

(58) Flynn, J. H.; Wall, L. A. General Treatment of the Thermogravimetry of Polymers. *J. Res. Natl. Bur. Stand., Sect. A*. **1966**, *70*, 478–523.

(59) Logvinenko, V. A.; Dybtsev, D. N.; Bolotov, V. A.; Fedin, V. P. Thermal Decomposition of Inclusion Compounds on the Base of the Metal–Organic Framework [Zn2(bdc)2(dabco)]. *J. Therm. Anal. Calorim.* **2015**, *121*, 491–497.

(60) Ziganshin, M. A.; Efimova, I. G.; Gorbatchuk, V. V.; Ziganshina, S. A.; Chuklanov, A. P.; Bukharaev, A. A.; Soldatov, D. V. Interaction of L-leucyl-L-leucyl-L-leucine Thin Film with Water and Organic Vapors: Receptor Properties and Related Morphology. *J. Pept. Sci.* **2012**, *18*, 209–214.

(61) Bérubé, C.; Cardinal, S.; Boudreault, P.-L.; Barbeau, X.; Delcey, N.; Giguère, M.; Gleeton, D.; Voyer, N. Novel Chiral N,N′-dimethyl-1,4-piperazines with Metal Binding Abilities. *Tetrahedron*. **2015**, *71*, 8077–8084.

(62) Gorbitz, C. H. Nanotube Formation by Hydrophobic Dipeptides. *Chem. - Eur. J.* **2001**, *7*, 5153–5159.

(63) Görbitz, C. H. Solvent Site Preferences in the Crystal Structures of L-leucyl-L-leucine Alcohol (1 : 1) Complexes. *Acta Chem. Scand.* **1998**, *52*, 1343–1349.

(64) Adhikari, B.; Palui, G.; Banerjee, A. Self-Assembling Tripeptide Based Hydrogels and Their Use in Removal of Dyes from Waste-Water. *Soft Matter*. **2009**, *5*, 3452–3460.

(65) Bellamy, L. J. *The Infra-Red Spectra of Complex Molecules*; Chapman and Hall: London, Wiley: New York, 1975.

(66) Cheam, T. C.; Krimm, S. Vibrational Analysis of Crystalline Diketopiperazine - I. Raman and I.R. Spectra. *Spectrochim. Acta*. **1984**, *40A*, 481–501.

(67) Miyazawa, T. Normal Vibrations of Monosubstituted Amides in the Cis Configuration and Infrared Spectra of Diketopiperazine. *J. Mol. Spectrosc.* **1960**, *4*, 155–167.

(68) In *NIST Chemistry WebBook;* Linstrom, P. J., Mallard, W. G., Eds.; NIST Standard Reference Database Number 69; National Institute of Standards and Technology: Gaithersburg, MD, http:// http://webbook.nist.gov, (retrieved July 10, 2017).

(69) Opfermann, J. Kinetic Analysis Using Multivariate Non-Linear Regression. I. Basic Concepts. *J. Therm. Anal. Calorim.* **2000**, *60*, 641–658.

(70) Govindaraju, T.; Pandeeswar, M.; Jayaramulu, K.; Jaipuria, G.; Atreya, H. S. Spontaneous Self-Assembly of Designed Cyclic Dipeptide (Phg-Phg) into Two-Dimensional Nano- and Mesosheets. *Supramol. Chem.* **2011**, *23*, 487–492.

TOC Graphic

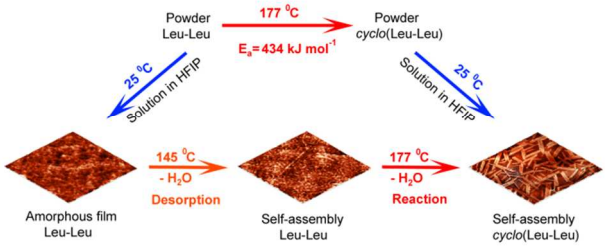
Powder
Leu-Leu
177 °C
E_a = 434 kJ mol^{-1}
Powder
cyclo(Leu-Leu)
25 °C
Solution in HFIP
25 °C
Solution in HFIP
145 °C
- H_2O
Desorption
177 °C
- H_2O
Reaction
Amorphous film
Leu-Leu
Self-assembly
Leu-Leu
Self-assembly
cyclo(Leu-Leu)

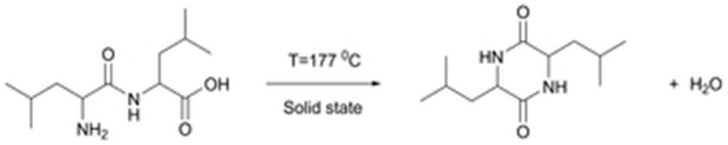

Figure 1. Scheme of the reaction of cyclization of Leu-Leu in the solid state.

15x2mm (600 x 600 DPI)

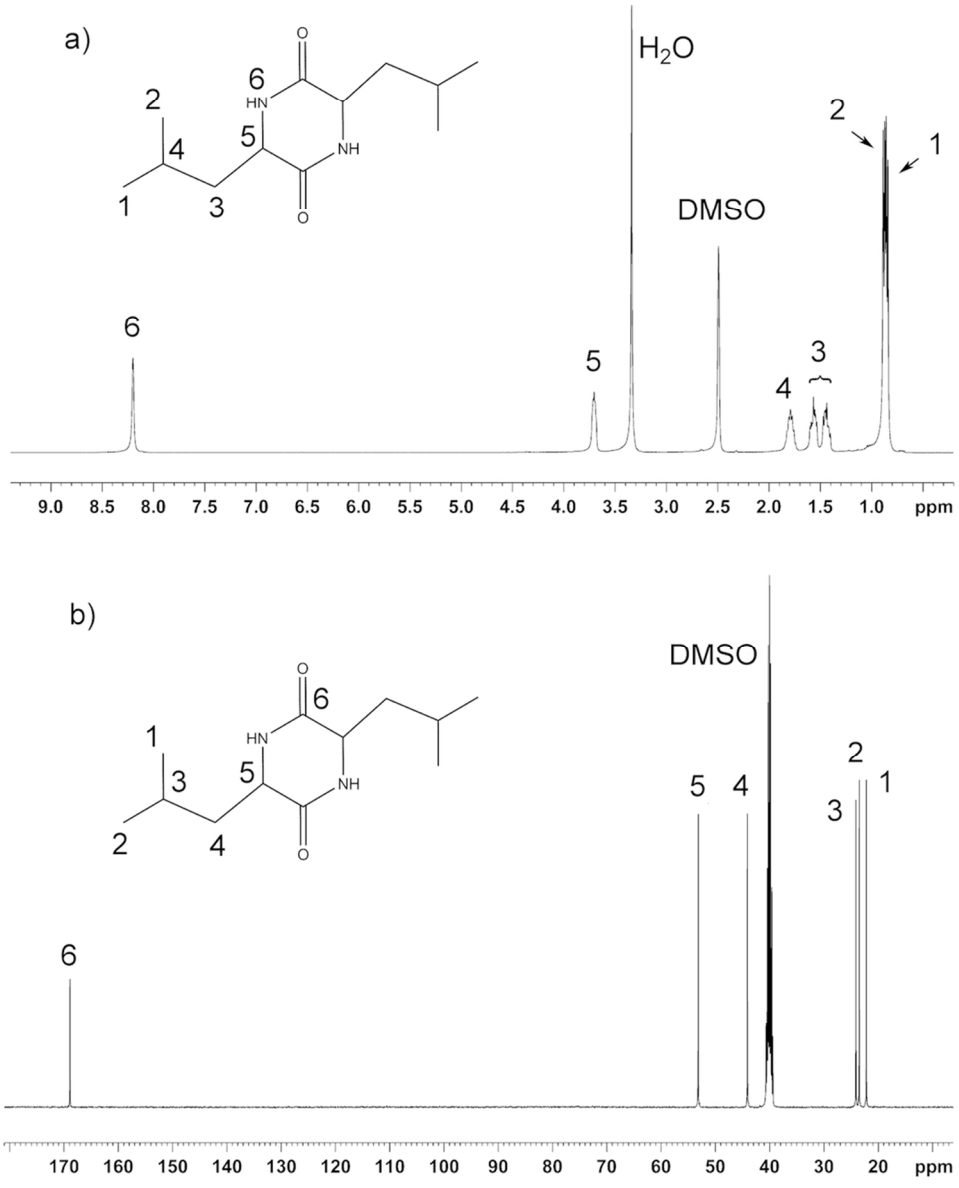

Figure 2. (a) ^{1}H NMR spectrum (400 MHz, DMSO-d_6) and (b) ^{13}C {^{1}H} NMR spectrum (100.6 MHz, DMSO-d_6) of *cyclo*(Leu-Leu).

99x123mm (300 x 300 DPI)

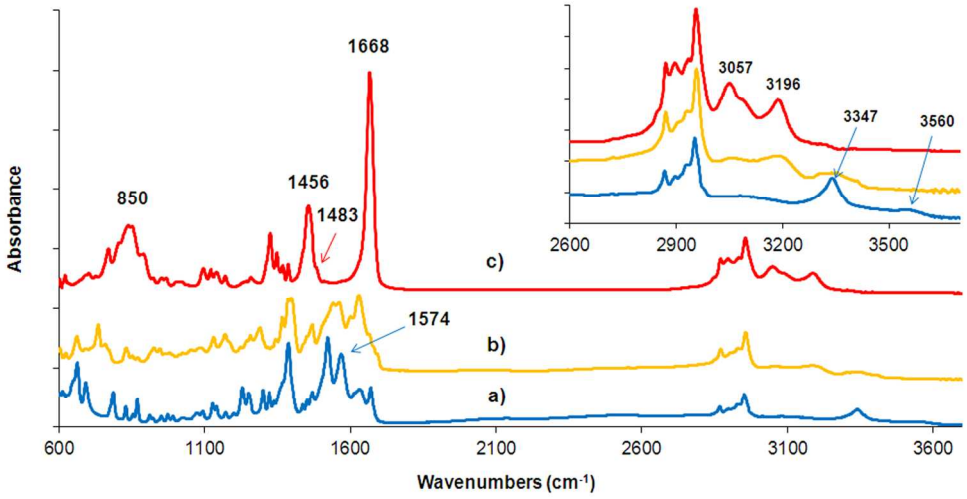

Figure 3. IR spectra at room temperature of powders of (a) initial Leu-Leu, (b) Leu-Leu after heating up to 145 °C and (c) Leu-Leu after heating up to 200 °C. The part of the spectrum in the range 2600-3700 cm^{-1} is shown in the inset.

140x70mm (300 x 300 DPI)

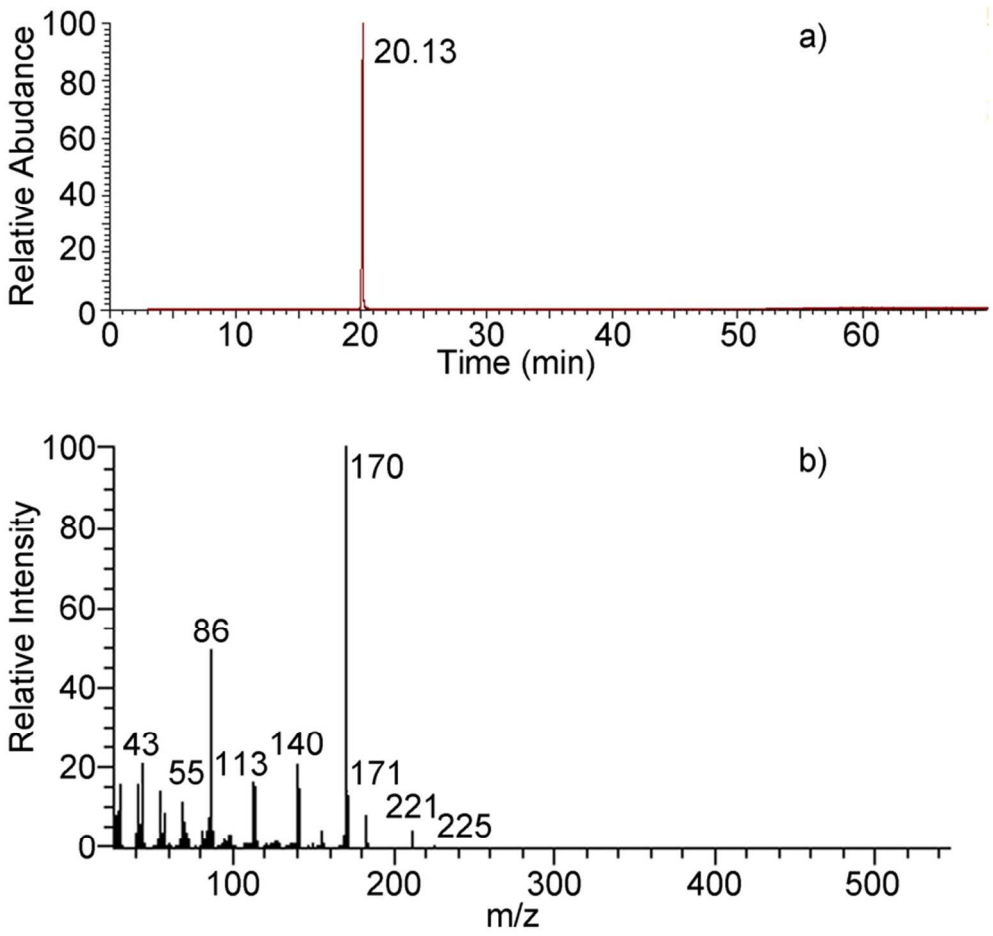

Figure 4. GC-MS of thermally induced powder of Leu-Leu up to 200 °C. (a) Data of GC, (b) data of MS.

80x75mm (300 x 300 DPI)

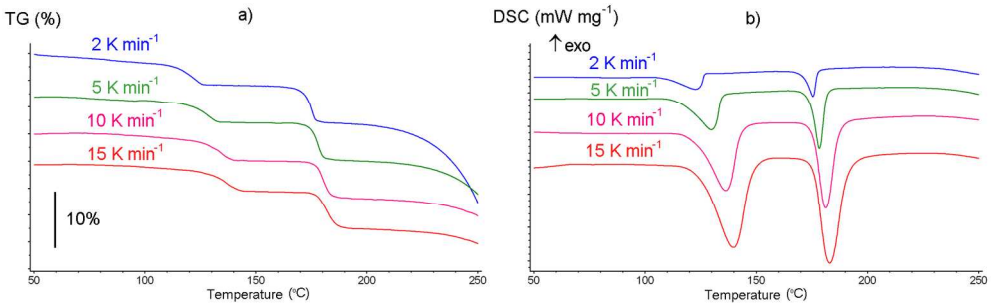

Figure 5. Data of (a) TG and (b) DSC analysis for Leu-Leu at different heating rates.

160x48mm (300 x 300 DPI)

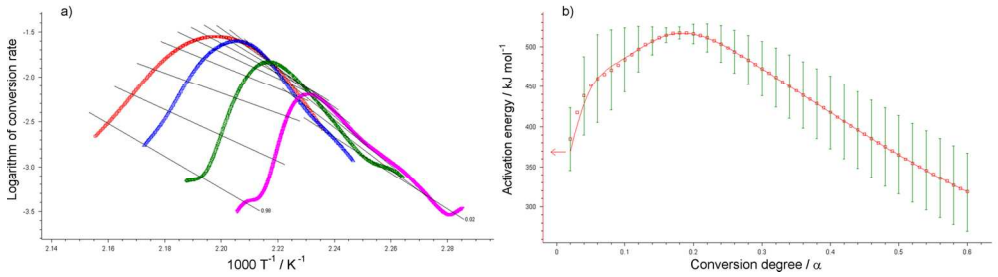

Figure 6. Friedman analysis of reaction of cyclization of Leu-Leu: (a) correlation of logarithm of conversion rate versus reciprocal temperature and (b) activation energies E_a versus degree of conversion α. Perpendicular lines show SD of calculation.

160x44mm (300 x 300 DPI)

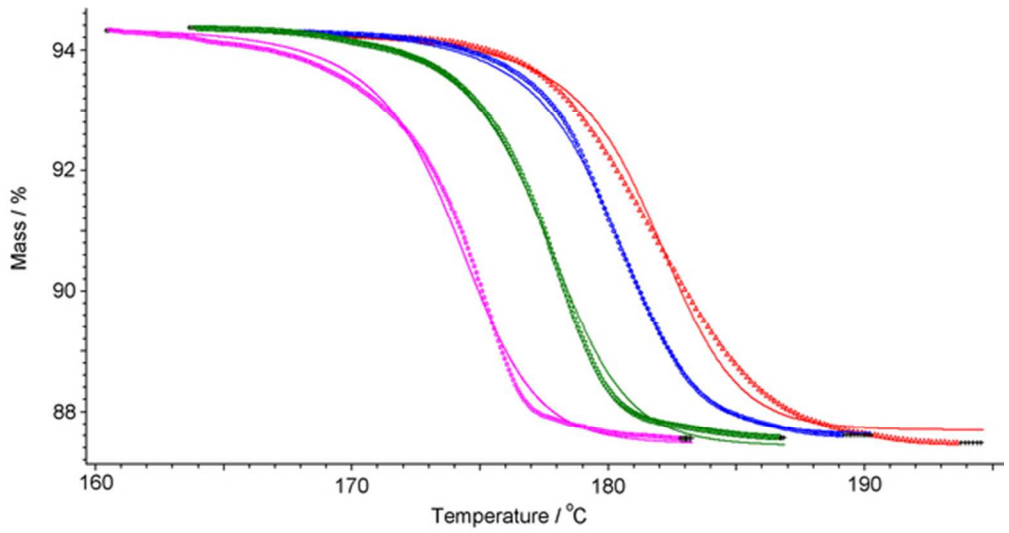

Figure 7. Correlation of experimental points from TG curves with the calculated lines in accordance with equation CnB.

53x28mm (300 x 300 DPI)

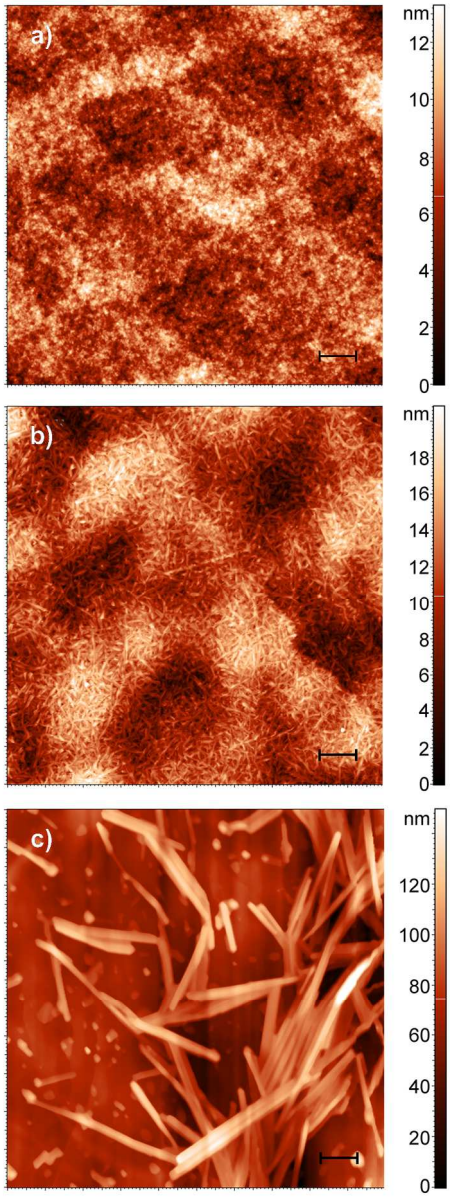

Figure 8. AFM images of the surface of (a) the initial Leu-Leu film deposited on the HOPG surface from a HFIP solution, (b) Leu-Leu film after heating up to 145 °C, (c) Leu-Leu film after heating up to 200 °C. Scale bar = 1 μm.

80x206mm (300 x 300 DPI)

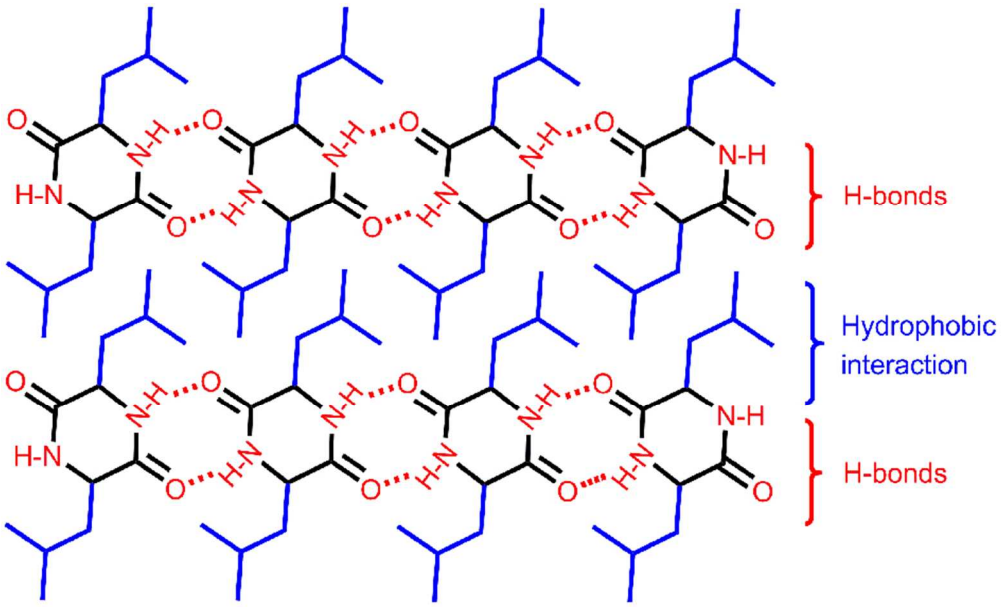

Figure 9. Scheme of possible organization of *cyclo*(Leu-Leu) in solid phase.

80x48mm (300 x 300 DPI)

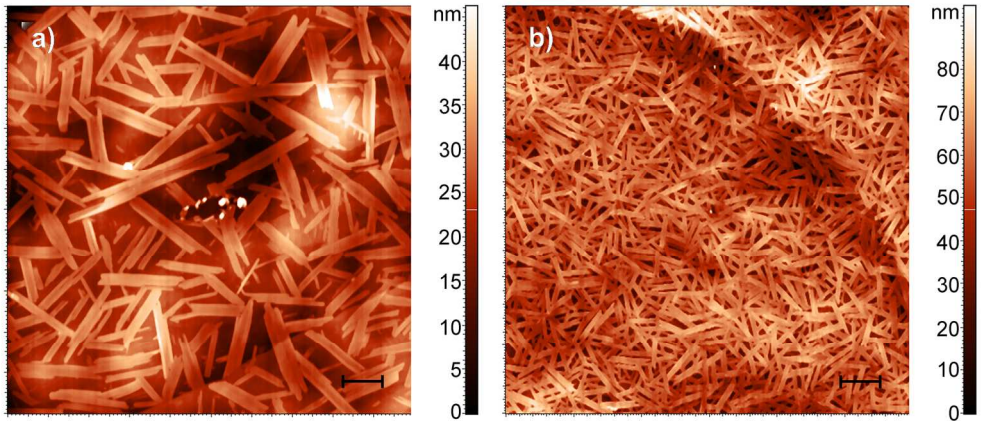

Figure 10. AFM images of the surface of film with the nanostructures obtained from solution of *cyclo*(Leu-Leu) in HFIP with different magnification. Scale bar = 3 μm (a) and 1 μm (b).

160x68mm (300 x 300 DPI)